

Phase-Imaging Ion-Cyclotron-Resonance Mass Spectrometry with the Canadian Penning Trap at CARIBU

D. Ray^{a,b,*}, A.A. Valverde^{a,b}, M. Brodeur^c, F. Buchinger^d, J.A. Clark^{b,a}, B. Liu^{c,b}, G.E. Morgan^{e,b}, R. Orford^f, W.S. Porter^c, G. Savard^{b,g}, K.S. Sharma^a, X.L. Yan^{b,h}

^a*Department of Physics and Astronomy, University of Manitoba, Winnipeg, MB, R3T 2N2, Canada*
^b*Physics Division, Argonne National Laboratory, Lemont, IL 60439, USA*

^c*Department of Physics and Astronomy, University of Notre Dame, Notre Dame, IN 46556, USA*

^d*Department of Physics, McGill University, Montreal, QC H3A 2T8, Canada*

^e*Department of Physics and Astronomy, Louisiana State University, Baton Rouge, LA 70803, USA*

^f*Nuclear Science Division, Lawrence Berkeley National Laboratory, Berkeley, CA 94720, USA*

^g*Department of Physics, University of Chicago, Chicago, IL 60637, USA*

^h*Institute of Modern Physics, Chinese Academy of Sciences, Lanzhou 730000, China*

Abstract

The Canadian Penning Trap mass spectrometer (CPT) has conducted precision mass measurements of neutron-rich nuclides from the California Rare Isotope Breeder Upgrade (CARIBU) of the Argonne Tandem Linac Accelerator System (ATLAS) facility at Argonne National Laboratory for over a decade, first using Time-Of-Flight Ion-Cyclotron-Resonance (TOF-ICR) and later using Phase-Imaging Ion-Cyclotron-Resonance (PI-ICR) techniques. Here we give an overview of the CPT system as it was operated for PI-ICR measurements at CARIBU for over half a decade, along with some recently studied systematic effects.

Keywords: Penning trap mass spectrometry, Phase-imaging ion-cyclotron-resonance

1. Introduction

Penning traps have been the most precise instruments for mass measurements of stable and radioactive nuclides for many different fields of physics for over four decades [1–3]. Penning trap mass spectrometry relies on determining the cyclotron frequency (ν_c) of an ion of mass M and charge q in a magnetic field B :

$$\nu_c = \frac{q}{2\pi M} B. \quad (1)$$

Once the ν_c of a target ion species and a calibrant (Cal.) ion species of known mass (for calibrating the B-field) are precisely measured, the atomic mass (m) of the target species is determined as,

$$m = \frac{q}{q^{\text{Cal.}}} \frac{\nu_c^{\text{Cal.}}}{\nu_c} (m^{\text{Cal.}} - q^{\text{Cal.}} m_e + B_e^{\text{Cal.}}) + q m_e - B_e, \quad (2)$$

*Corresponding author: dray@triumf.ca; Current Address: TRIUMF, 4004 Wesbrook Mall, Vancouver, BC V6T 2A3, Canada

where m_e is the mass of an electron, and $B_e^{\text{Cal.}}$ and B_e are the electron binding energies of the calibrant and the target species.

The Canadian Penning Trap (CPT) system was designed and commissioned at the Tandem Accelerator Superconducting Cyclotron (TASCC) facility at Chalk River Laboratories in Ontario, Canada [4] in the late 90s. Upon the decommissioning of TASCC, the CPT was moved to Argonne National Laboratory (ANL) [5] in 2001 and was set up in the “Triangle Room” experimental area at the Argonne Tandem Linac Accelerator System (ATLAS) facility [5]. Upon the completion of the CAliifornium Rare Isotope Breeder Upgrade (CARIBU) [6] at the ATLAS facility in 2011, the CPT was moved there [7]. Since then, it has been used to conduct precision mass measurements of neutron-rich nuclides produced at CARIBU focusing on probing the astrophysical rapid neutron capture process (r process) [8, 9] and nuclear structure features among the rare-earth nuclides [10, 11], first using Time-of-Flight Ion-Cyclotron-Resonance (TOF-ICR) [12] and then using Phase-Imaging Ion-Cyclotron-Resonance (PI-ICR) [13, 14] techniques. This fruitful period ended with its decommissioning in 2023, prior to its move to the upcoming N=126 Factory [15] at ANL. This paper discusses the CPT system as it was operated for PI-ICR in CARIBU for over half a decade, along with some new systematic studies.

2. The CARIBU facility

CARIBU is a unique facility which produces neutron-rich nuclides by collecting the spontaneous fission fragments from a ^{252}Cf source, which are sent as low-energy beams either to the CARIBU low-energy experimental area where the CPT resided or the newly constructed Area 1, or to the Electron Beam Ion Source (EBIS) [16] for charge-breeding and acceleration before injection into ATLAS for other experiments. At the heart of CARIBU is a ~ 0.5 Ci ^{252}Cf source decaying with a half-life of 2.645(8) years and having a spontaneous fission branch of 3.1028(7)% [17]. The fission fragments pass through a gold degrader foil and enter a large volume gas catcher [18] consisting of a cylindrical body and a cone. Here they are stopped and thermalized in high-purity He gas, and are extracted using a combination of gas flow, and radio-frequency (RF) and direct current (DC) fields with $q = 1+$ or $2+$. The gas catcher and associated radio-frequency quadrupole (RFQ) ion guides sit on a 36 kV high voltage (HV) platform. The extracted ions first undergo mass-selection on the basis of their mass numbers (A) and q by passing through the isobar separator [19] consisting of a pair of dipole magnets and operated at a resolving power of 5,000, before they are cooled and bunched using a RFQ cooler-buncher. The bunched beam is extracted at 3 keV every 50 ms or 100 ms, and then gets further mass-resolved by a multi-reflection time-of-flight (MR-TOF) mass separator [20]. For most CPT experiments, the ions are cycled inside the MR-TOF for 15 – 20 ms, enabling achievement of a mass resolution of 100,000. At the exit of the MR-TOF, the mass-resolved beam passes through a Bradbury-Nielson gate (BNG), where the target nuclides are precisely selected on the basis of their TOF and sent to the CPT system.

All the beamline components downstream from the buncher require triggering at the precise times when the bunched beam approaches them. The trigger signals are all initiated by the ions’ ejection from the buncher. The signals for all the components except the BNG are fine-tuned to the A/q of the ions in the beam, while the BNG trigger is fine-tuned to the precise m/q of the target nuclide.

3. The CPT system

3.1. Overview

The CPT system consists mainly of two sections, a stable-ion-source (SIS), an elevator drift tube and a linear Paul trap (LT) constituting the lower, beam-preparation section, and a precision Penning trap, the CPT, equipped with a position-sensitive microchannel plate detector (PS-MCP, also known as MCP 5) making up the upper measurement section. The sections are housed in a ~ 4.5 m tower structure as shown in Fig. 1. The system also includes a host of other components like diagnostic silicon surface barrier (Si) and MCP detectors, turbomolecular pumps (TP) and standard electrostatic beamline components, some of which have been excluded from the figure for simplicity. The lower section is maintained at high vacuum ($10 \mu\text{Torr}$ to 100nTorr) while the upper section is maintained at ultra-high vacuum ($< 1 \text{nTorr}$) as required for precision measurement. The whole system can be isolated from CARIBU using a gate valve V2, while V6 separates the upper and lower sections.

3.2. Offline stable ion source (SIS)

The SIS is located at the bottom of the tower between the valve V2 and the first diagnostic station of the CPT system “Si/MCP0”, as can be seen in Fig. 1. It consists of a mixed-alkaline, surface-ionization ion source (Model 101139) from Heat Wave Labs [21], containing salts of natural-abundance Cs, Rb and K in roughly equal proportions, and heated using a pair of coaxial heating elements. This produces continuous ion streams of $^{133}\text{Cs}^+$, $^{85,87}\text{Rb}^+$, and $^{39,41}\text{K}^+$, which are accelerated into the main beamline, and used for optimizing the different beamline components and magnetic-field calibration during precision measurement campaigns due to their precisely known masses [22].

3.3. Beam preparation : Elevator and linear Paul trap

The traps (LT and CPT) are designed to operate at low voltages, and to trap and manipulate ions with near-zero energies. Therefore, the ~ 3 keV energy of the incoming beam from CARIBU needs to be lowered. This is accomplished using an elevator that consists of a 30 cm long drift tube. A signal mirroring the BNG trigger is used to trigger a delayed pulse which lowers the potential of the elevator from ground to ~ -3 kV when the ion bunch is inside it. Ions from the SIS are extracted at the transport voltage of the tower and do not require the elevator. Therefore, the elevator voltage is maintained at the standard transport voltage of the system for SIS beam.

The LT is a gas-filled linear RFQ Paul trap, used as a buffer trap to make operation of the system more general. The segmented RFQ electrode structure is cooled by circulating liquid nitrogen, using a custom-made pump [23], to reduce thermal excitations and it is filled with high-purity He gas at $\sim 10 \mu\text{Torr}$. After injection into the LT, ions are trapped, using a combination of radial RF fields and an axial DC potential well, and cooled via collisions with the He gas for a minimum of 30 ms reducing their emittance, before they are ejected towards the CPT.

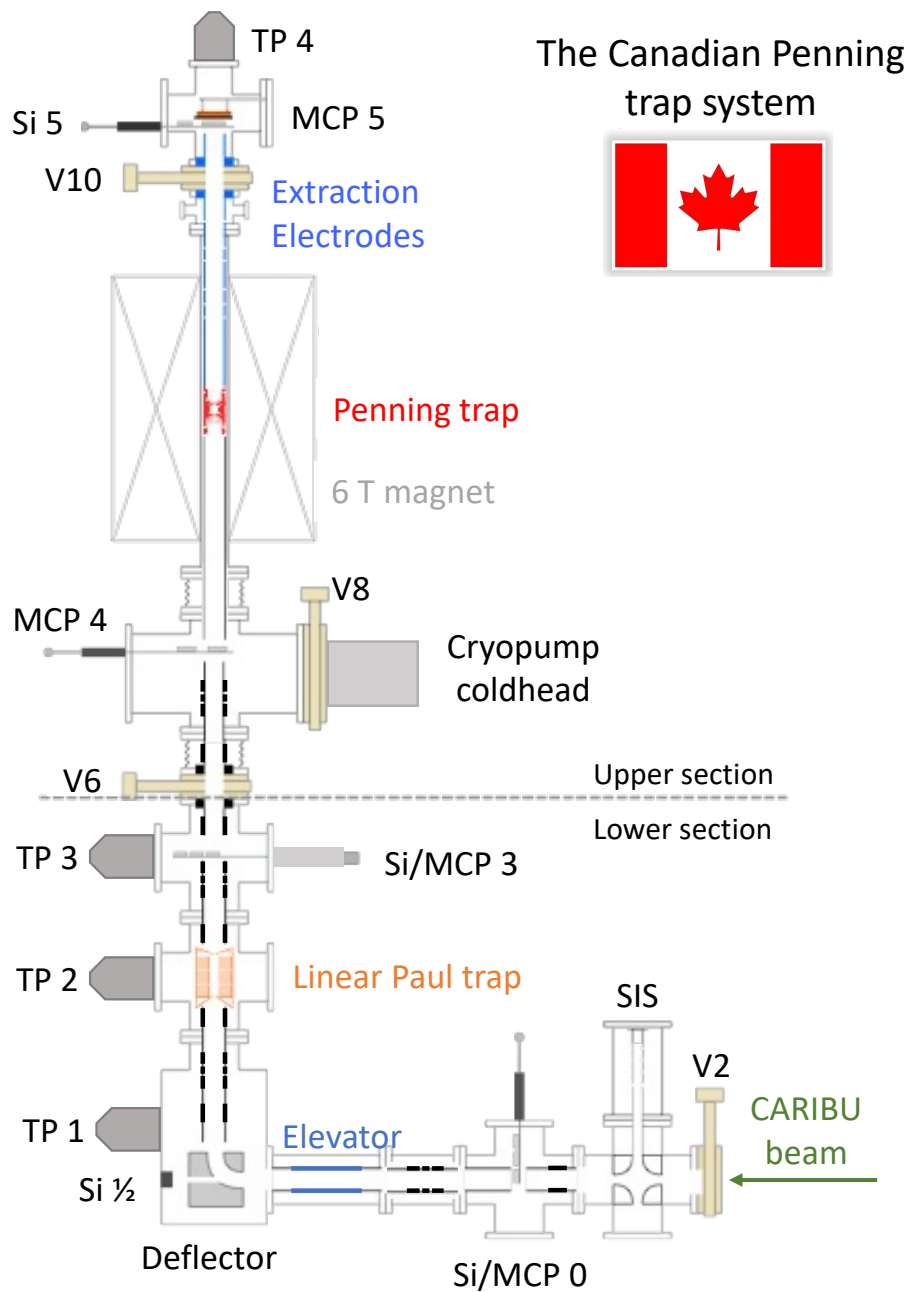


Figure 1: Schematic diagram of the CPT tower (not to scale), showing the major components.

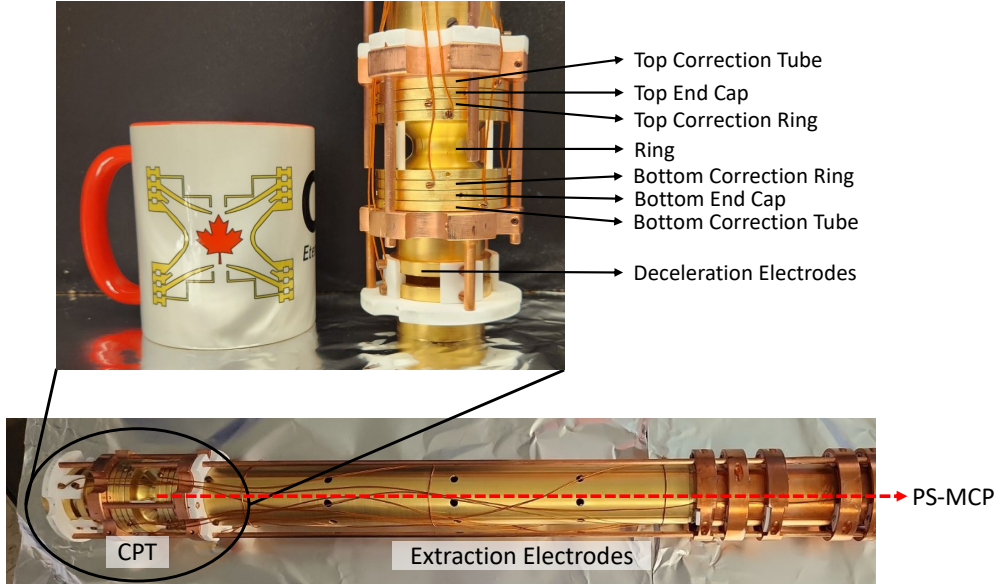


Figure 2: The CPT electrode assembly showing the trap (zoomed in on the inset, with a mug added for scale) and the extraction electrodes. An ion's path from the trap towards the PS-MCP is shown with the red dotted line.

3.4. Penning trap

The Canadian Penning Trap [4] is a hyperboloid Penning trap with characteristic dimensions of $r_0 = 11.6$ mm and $z_0 = 10$ mm consisting of ten electrodes: pairs (top and bottom) of correction tubes, end caps and correction rings, on either side of a 4-segment ring electrode. There are two 5-mm apertures on both sides through the end cap and correction tube electrodes for entry and exit of the ions. The correction electrodes are used to compensate for the non-ideal or practical aspects in the trap design, like the segmented ring, the finite size of the electrodes and the apertures, and create a harmonic electric potential. The trap sits inside the bore of a 6 T superconducting magnet and forms one physical assembly together with a pair of deceleration injection electrodes upstream and nine cylindrical extraction drift tubes downstream [5]. This is shown in Fig. 2. All the trap electrodes are made with gold-plated, oxygen-free high-purity copper (OFHC) with Macor[®] insulators to satisfy the electric conductivity, magnetic susceptibility and UHV requirements. During the transfer between the LT and the CPT, some energy spread is imparted in the ion cloud. Therefore once the ions are captured, an evaporative cleaning procedure is conducted to remove the high energy ions, and ensure that the trapped cloud sits at the center of the trap, always probing the same B field. Next, RF excitations are applied to the ring electrode as required for mass measurement using PI-ICR, after which the ions are ejected from the trap. PI-ICR depends on accurate projections of the ions' in-trap positions on to the PS-MCP. To minimize distortions and optimize the quality of this projection, the ions' TOF through the B field gradient from the trap to the detector had to be minimized. As part of the ejection procedure, the drift tube closest to the trap, in a region of large B field gradient, is pulsed thereby accelerating

the ions without perturbing the harmonicity of the trap. The rest of the drift tubes are maintained at a fixed negative potential as the ions are transferred towards the PS-MCP. The detector setup is a commercial package from RoentDek Handels GmbH. The detector setup is a commercial package from RoentDek Handels GmbH, and includes the PS-MCP (DLD40), consisting of a pair of image quality MCP plates (front and back), with a delay line anode, along with associated electronics comprising of a signal decoupling feedthrough (FT12TP), a fast signal amplifier (FAMP6), a constant fraction discriminator (CFD4c), a high resolution time-to-digital converter (TDC8HP), and readout software (CoboldPC). Each MCP plate has an active diameter of 45 mm and thickness of 1.5 mm. The set up provides an electron gain of 10^7 for a voltage difference of -2400 V across the two MCP plates, with a position resolution of < 0.1 mm, temporal resolution of < 0.2 ns, rate capability of 1 MHz and multihit dead time of $10 - 20$ ns for each ion-hit [24].

4. Mass measurement : Phase-imaging ion-cyclotron resonance (PI-ICR)

PI-ICR relies on determining a nuclide's ν_c by obtaining the phases corresponding to the ions' magnetron (ν_-) and reduced cyclotron (ν_+) radial eigenmotions acquired over periods of no excitation. The details of PI-ICR implementation at the CPT are described in Ref. [14]. In short, ν_c is determined by directly measuring the sum of ν_+ and ν_- . One ν_c measurement cycle consists of two phase measurements: a reference phase (ϕ^{ref}) and a final phase (ϕ^{final}). Each of these phase measurements involves application of three RF excitations for each trap cycle: a ν_- dipole centering pulse, a ν_+ dipole pulse to increase the radius of the corresponding motion and excite the ions to an orbit, and finally a ν_c quadrupole pulse to convert the ions' fast ν_+ motion to the slow ν_- motion for detection before they are ejected from the trap. This is repeated for multiple trap cycles to obtain enough ion-hits forming spots corresponding to the measured reference or final phase. The total trap time, the durations of all three excitations, and timing structure of the two dipole excitations are kept the same for both the reference and the final phase measurements. The time of application of the ν_c pulse differentiates ϕ^{ref} and ϕ^{final} . For the reference phase, the ν_c pulse is applied right after the end of the ν_+ pulse, so the ions only acquire ν_- phase in the time (T) between the conversion and the ejection pulse. As a result, the reference spot is always a single spot. For the final phase, there is a delay (t_{acc}) between the two pulses, and the ions accumulate a combination of strongly mass-dependent ν_+ phase over time t_{acc} , and ν_- phase over time $T - t_{\text{acc}}$. This means all beam species get resolved over a large-enough t_{acc} for the final spots. Each reference and final spot is clustered and fitted using techniques described in Ref. [25, 26] to obtain the corresponding *spot-centroids* and hence the acquired phases. The phase difference $\phi_{\text{total}} = \phi^{\text{final}} - \phi^{\text{ref}}$ can then be determined, and from it, one can obtain ν_c as:

$$\nu_c = \frac{\phi_{\text{total}}}{2\pi t_{\text{acc}}} = \frac{\phi_c + 2\pi N}{2\pi t_{\text{acc}}} , \quad (3)$$

where ϕ_c is the phase excess after completion of N complete cyclotron revolutions in time t_{acc} . This is shown in Fig. 3. Once the ν_c of the target nuclide has been measured, ν_c of a calibrant species with well-known mass is measured using the same parameters to calibrate the B field, and the mass of the target ion is determined using Eq. 2. It should

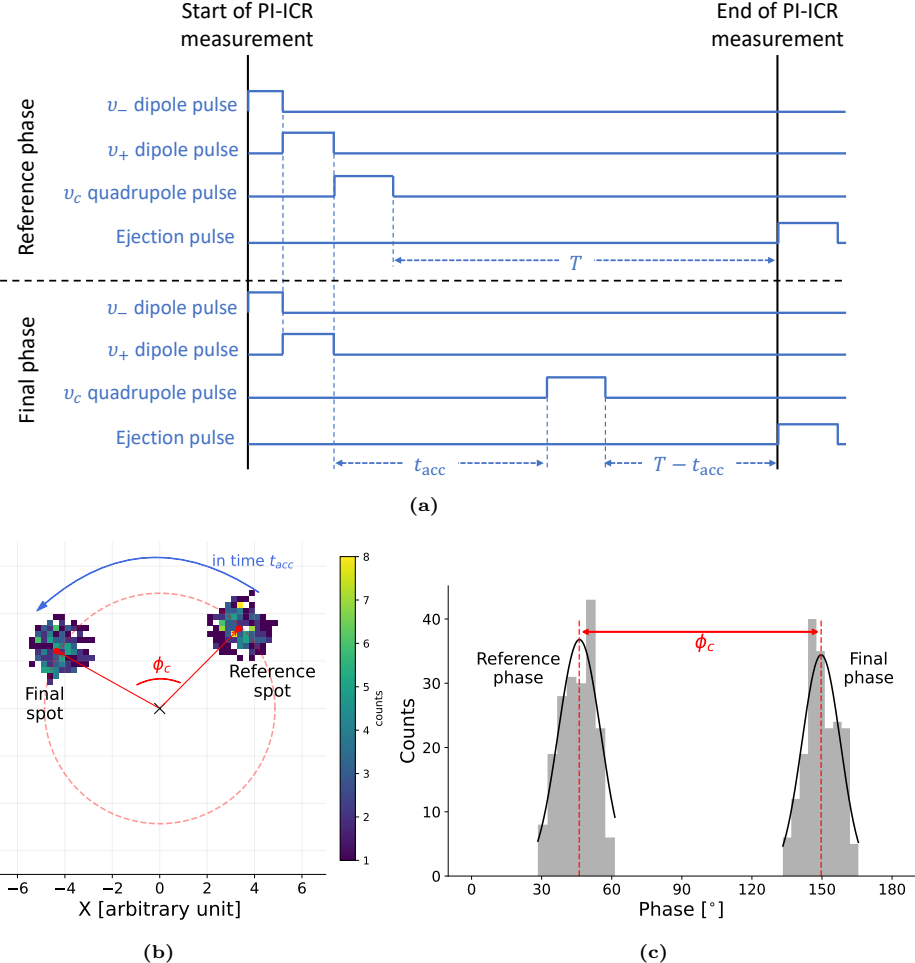


Figure 3: Illustration of the PI-ICR technique used at the CPT. Panel (a) shows the RF excitation schemes used during a PI-ICR measurement of reference (top) and final (bottom) phases. In panel (b), reference and final spots are shown superimposed on one spectrum. The ions acquire an excess phase shown by the angle ϕ_c between the reference to the final spot in time t_{acc} . The *spot-centroids*, obtained from clustering and fitting [25, 26], is shown by the red dots, while the trap center is denoted by a black cross. The red dotted circle represents a hypothetical revolution-path the ions take post their excitement by the ν_+ dipole pulse. In panel (c), the corresponding phase projections are shown along with fits to the data.

be noted here that the electron binding energies for isotopes measured at the CPT are usually of the order of 1-10s of eV, over an order of magnitude smaller than the precision of the measured masses, and are therefore ignored.

4.1. Improving accuracy of PI-ICR measurements

The main factors that affect accuracy in PI-ICR measurements at the CPT include ensuring the target and calibrant ions probe the same magnetic field, a harmonic electric field and resolution of PI-ICR spots. Effects relating to magnetic field inhomogeneities are minimized by fine-tuning the injection pulse and conducting an evaporative cleaning routine. With this procedure, the ions upon injection always get confined at the center of the trap in the axial direction where the B-field is largely homogeneous ($\Delta B \sim 0.1 \mu\text{T}/\text{mm}$).

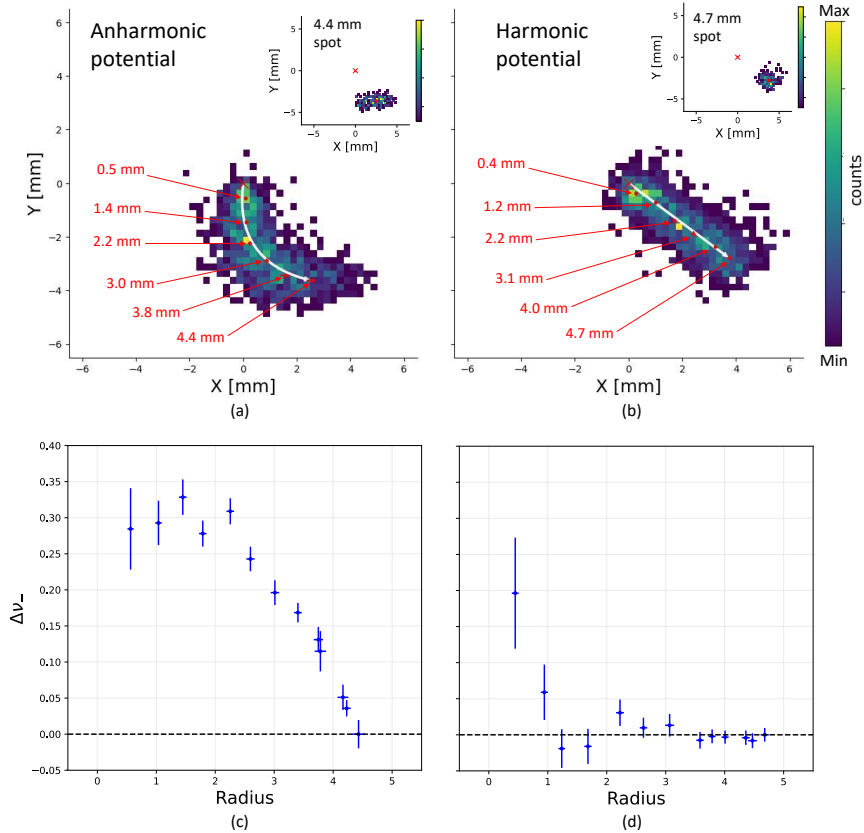


Figure 4: Creating a harmonic trap potential by tuning the correction tube potential. Left: an untuned correction tube potential leading to an anharmonic electric field causing a misalignment in the ν_- spots at different radii and smearing of the spots (outermost spot shown on the inset) (in panel (a)), and the corresponding shifts in ν_- (in panel (c)). Right: A tuned correction tube potential making the electric field harmonic and leading to aligned spots, with the outermost spot shown on the inset (panel (b)), and corresponding $\Delta\nu_-$ (panel (d)).

While ν_c has no direct dependence on the trap's electric field, its measurement using PI-ICR depends on the harmonicity, due to the dependence of ν_+ and ν_- on the

electric field. The electric field harmonicity of the trap can be optimized using PI-ICR measurements. If the ions are excited to different radii by applying ν_+ excitations over same duration but with different peak-to-peak voltage, and individual reference or ν_- phase measurements are conducted at each radii, a harmonic electric potential would mean an unchanged ν_- frequency that is independent of the radius. This will also lead to a radial alignment of the reference spots. On the other hand, a non-harmonic electric field would lead to a radius dependence of ν_- and distortion of the PI-ICR spots [13]. The correction tube electrodes can be used to correct for the octupolar and dodecapolar imperfections in the trapping potential [27, 28] and make the potential harmonic. This is shown in Fig. 4 for an anharmonic (panels (a) and (c) to the left) and a harmonic (panels (b) and (d) to the right) electric potential. The top panels, (a) and (b), show a few selected reference spots at different radii with the outer most spots, typically used for mass measurement, shown on the inset. The corresponding shifts in the measured ν_- with respect to the outermost spot are shown in the bottom panels (c) and (d). As can be seen from the inset of Fig. 4 (a) and (b), a harmonic potential well will also lead to an undistorted spot-like image on the detector.

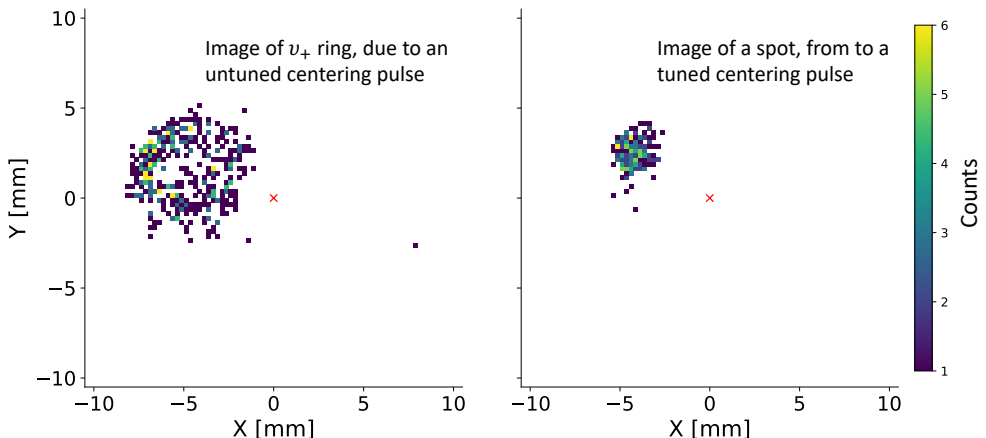


Figure 5: Improvement in spot resolution by tuning the centering pulse. Left: An initial ν_- motion from an untuned centering pulse gets converted to a ν_+ motion before ejection and gets imaged as a ring. Right: A tuned centering pulse minimizing the initial ν_- motion leading to observation of a spot-image at an orbit. The trap center is marked by the red cross.

The ν_- dipole ‘centering’ pulse ensures that the ions are perfectly centered before they are excited to a radius by the ν_+ dipole pulse. An untuned centering excitation means the ions would possess a significant initial ν_- motion which continues after the ν_+ excitation and gets converted to the fast ν_+ motion by the ν_c pulse prior to ejection. As a result, the observed image becomes that of a ring instead of a spot. This is shown in Fig. 5, where a four-parameter tuning of the amplitude, phase, duration and time-of-application of the ν_- pulse ensured detecting the image of a spot (right) instead of a ring (left). It should be mentioned here that a well-tuned ν_- pulse means a negligible but non-zero initial ν_- motion which is adequate for spot optimization purposes, but is not sufficient to eliminate the *sine-fit* systematic effect described in Ref. [14].

4.2. Systematic Effects

A number of systematic effects present in the PI-ICR implementation at the CPT and methods to address them have been previously discussed in Ref. [14], and continued to be studied. This includes the effects arising from a non-circular projection from the trap onto the detector, which following the procedures outlined in Ref. [14] is limited to less than 2 ppb in $\Delta\nu_c/\nu_c$. A dependence of measured ν_c on t_{acc} , due to the negligible but non-zero initial ν_- motion of the ions prior to the application ν_+ excitation has been observed at the CPT [14]. This is corrected by conducting a series of ν_c measurements by varying t_{acc} over at least one ν_- period, and then fitting the data to the *sine-fit* model described in Ref. [14] to obtain the true ν_c . Shifts in measured ν_c due to presence of close-mass contaminant species in the beam during measurement are corrected by applying a phase-correction, as stated in Ref. [14], and this has resulted in changes of less than 2 ppb. Since then, a few other effects, typically observed in Penning trap mass spectrometry, have been studied, and the findings are presented here.

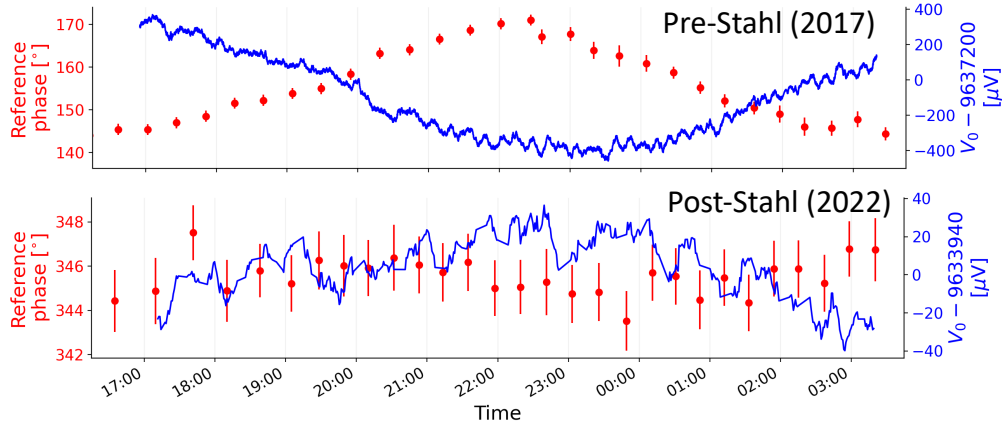


Figure 6: Improvement in stability of the trap depth (V_0) and corresponding ϕ^{ref} -drifts over 10 hours with the installation of the Stahl voltage supply

It can be shown that ν_- is proportional to V_0/B , where V_0 is the depth in the trapping potential, given by the potential difference between the end cap and the ring electrodes. Since, ϕ^{ref} is primarily a ν_- phase that the ions acquire over time T , the stability of the trap power supply is of paramount importance for precision measurements using PI-ICR. This effect was briefly discussed in Ref. [14], and could lead to mass shifts of up to ~ 0.1 ppm in extreme cases. The “new” power supply mentioned in Ref. [14], an ultra-high precision voltage supply from Stahl Electronics (4 channel, ± 14 V BS Series) [29] with extremely low temperature dependency ($10^{-6} \Delta V/V$ per Kelvin) and temporal voltage fluctuations ($< 10^{-7} \Delta V/V$ per minute), has since been thoroughly tested and is currently used as a dedicated supply to bias the trap electrodes. The improvement in stability from this Stahl power supply is shown in Fig. 6. Before the installation of this new power supply, a $\sim 25^\circ$ shift in ϕ^{ref} could be acquired over a ~ 685 ms duration, and now, it has been reduced to $\sim 3^\circ$ over a similar timeframe. As an additional precaution, reference data is acquired every few minutes or once per final file,

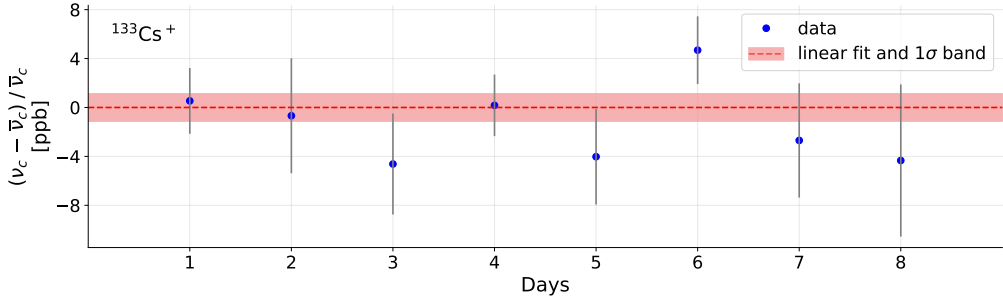


Figure 7: Temporal drift of the magnetic field over 8 days shown as a relative difference in the measured cyclotron frequencies from a weighted average value in ppb.

then either the reference closest in time to a final file is considered for that final file, or extrapolated *true* references are determined and used. This has allowed for trapping the ions over larger times (~ 1 s) while keeping the effects of electric field instabilities to less than 2 ppb, and achieving precisions of a few ppb in mass measurements [25, 30, 31].

As can be seen from Eq. 1, stability of the trap's B field is critical for accurate measurements. Spatial drifts are addressed by ensuring the ions probe the same B field in all three dimensions. Temporal drifts are handled by doing a field-calibration as close in time as possible to a target-nuclide measurement. Figure 7 shows results of ν_c -measurements conducted to gauge the stability of the B-field using $^{133}\text{Cs}^+$ ions. The study was done over a period of eight days, which is the typical duration of experimental campaigns at the CPT. The measured cyclotron frequencies were found to vary statistically with a standard deviation of 1.2 ppb. Additionally, several calibrant measurements with ions from CARIBU and SIS are interleaved in between target-nuclide measurements.

The effect of ion-ion interaction is kept to a minimum by keeping the ion-rate low, and later imposing an *ion-cut*¹ condition in the offline data analysis of both the target and the calibrant species. A count class analysis using $^{133}\text{Cs}^+$ ions from SIS was conducted by varying the current for heating the source and hence the ion-rate, collecting high-statistics datasets, and applying different ioncuts in the analysis. It was seen that by considering only < 5 simultaneously detected ion-hits on the PS-MCP, the effect of ion-ion interaction can be restricted to within 1 ppb.

All masses recently measured and reported were determined following these, in addition to the procedures of Ref. [14]. The uncertainty from the *sine-fit* systematic was incorporated in the statistical uncertainty of measurement, while that due to contaminant species was propagated from the individual components in the calculation. Furthermore, a systematic contribution of 3.2 ppb was added in quadrature to the statistical uncertainties to account for possible shifts due to magnetic field drifts, electric field instabilities, ion-ion interactions, and non-circular projection from the trap to the detector.

¹ *ion-cut* considers only the data involving a user-defined range for number of ion-hits detected simultaneously on the PS-MCP.

5. Outlook

PI-ICR implementation at the CPT at CARIBU has been a fruitful endeavour measuring masses of more than 200 neutron-rich nuclides, resulting in multiple publications and theses over six years. PI-ICR has increased the measurement sensitivity of the CPT helping achieve ppb-level precision [25, 30, 31] and record mass resolving power of $\sim 10^7$ [32], and allowing for measurement of some of the most weakly populated ^{252}Cf -fission fragments [8, 25]. The CPT system is currently being transported to the upcoming N=126 Factory [15] in ATLAS at ANL. Multiple upgrades, including a revamp of the control system and introduction of a Lorentz steerer [33] just before the trap for efficient on-center injection into the trap are planned. Although this marks the end of the CPT-at-CARIBU project, it points towards an exciting future in studying neutron-rich nuclides far from stability.

References

- [1] G. GÄrtner, E. Klempt, **A direct determination of the proton-electron mass ratio**, Zeitschrift für Physik A Atoms and Nuclei 287 (1) (1978) 1–6. doi:[10.1007/BF01408352](https://doi.org/10.1007/BF01408352).
URL <https://doi.org/10.1007/BF01408352>
- [2] H.-J. Kluge, **Penning trap mass spectrometry of radionuclides**, International Journal of Mass Spectrometry 349–350 (2013) 26–37, 100 years of Mass Spectrometry. doi:<https://doi.org/10.1016/j.ijms.2013.04.017>
URL <https://www.sciencedirect.com/science/article/pii/S1387380613001449>
- [3] K. Blaum, **High-accuracy mass spectrometry with stored ions**, Physics Reports 425 (1) (2006) 1–78. doi:<https://doi.org/10.1016/j.physrep.2005.10.011>.
URL <https://www.sciencedirect.com/science/article/pii/S0370157305004643>
- [4] G. Savard, R. Barber, D. Beeching, F. Buchinger, J. Crawford, S. Gulick, X. Feng, E. Hagberg, J. Hardy, V. Koslowsky, J. Lee, R. Moore, K. Sharma, M. Watson, **The Canadian Penning trap mass spectrometer**, Nuclear Physics A 626 (1) (1997) 353–356, proceedings of the Third International Conference on Nuclear Physics at Storage Rings. doi:[https://doi.org/10.1016/S0375-9474\(97\)00557-5](https://doi.org/10.1016/S0375-9474(97)00557-5)
URL <https://www.sciencedirect.com/science/article/pii/S0375947497005575>
- [5] G. Savard, R. C. Barber, C. Boudreau, F. Buchinger, J. Caggiano, J. Clark, J. E. Crawford, H. Fukutani, S. Gulick, J. C. Hardy, A. Heinz, J. K. P. Lee, R. B. Moore, K. S. Sharma, J. Schwartz, D. Seweryniak, G. D. Sprouse, J. Vaz, **The Canadian Penning Trap Spectrometer at Argonne**, in: D. Lunney, G. Audi, H.-J. Kluge (Eds.), **Atomic Physics at Accelerators: Mass Spectrometry**, Springer Netherlands, Dordrecht, 2001, pp. 223–230. doi:https://doi.org/10.1007/978-94-015-1270-1_18
- [6] G. Savard, S. Baker, C. Davids, A. Levand, E. Moore, R. Pardo, R. Vondrasek, B. Zabransky, G. Zinkann, **Radioactive beams from gas catchers: The CARIBU facility**, Nuclear Instruments and Methods in Physics Research Section B: Beam Interactions with Materials and Atoms 266 (19–20) (2008) 4086–4091.
URL <https://www.sciencedirect.com/science/article/abs/pii/S0168583X08006848?via%20ihub>
- [7] J. Van Schelt, D. Lascar, G. Savard, J. A. Clark, P. F. Bertone, S. Caldwell, A. Chaudhuri, A. F. Levand, G. Li, G. E. Morgan, R. Orford, R. E. Segel, K. S. Sharma, M. G. Sternberg, **First Results from the CARIBU Facility: Mass Measurements on the *r*-Process Path**, Phys. Rev. Lett. 111 (2013) 061102. doi:[10.1103/PhysRevLett.111.061102](https://doi.org/10.1103/PhysRevLett.111.061102)
URL <https://link.aps.org/doi/10.1103/PhysRevLett.111.061102>
- [8] R. Orford, N. Vassh, J. A. Clark, G. C. McLaughlin, M. R. Mumpower, G. Savard, R. Surman, A. Aprahamian, F. Buchinger, M. T. Burkey, D. A. Gorelov, T. Y. Hirsh, J. W. Klimes, G. E. Morgan, A. Nystrom, K. S. Sharma, **Precision mass measurements of neutron-rich neodymium and samarium isotopes and their role in understanding rare-earth peak formation**, Phys. Rev. Lett. 120 (2018) 262702. doi:[10.1103/PhysRevLett.120.262702](https://doi.org/10.1103/PhysRevLett.120.262702)
URL <https://link.aps.org/doi/10.1103/PhysRevLett.120.262702>

- [9] R. Orford, N. Vassh, J. A. Clark, G. C. McLaughlin, M. R. Mumpower, D. Ray, G. Savard, R. Surman, F. Buchinger, D. P. Burdette, M. T. Burkey, D. A. Gorelov, J. W. Klimes, W. S. Porter, K. S. Sharma, A. A. Valverde, L. Varriano, X. L. Yan, [Searching for the origin of the rare-earth peak with precision mass measurements across ce-eu isotopic chains](#), Phys. Rev. C 105 (2022) L052802. [doi:10.1103/PhysRevC.105.L052802](https://doi.org/10.1103/PhysRevC.105.L052802)
 URL <https://link.aps.org/doi/10.1103/PhysRevC.105.L052802>
- [10] D. J. Hartley, F. G. Kondev, R. Orford, J. A. Clark, G. Savard, A. D. Ayangeakaa, S. Bottoni, F. Buchinger, M. T. Burkey, M. P. Carpenter, P. Copp, D. A. Gorelov, K. Hicks, C. R. Hoffman, C. Hu, R. V. F. Janssens, J. W. Klimes, T. Lauritsen, J. Sethi, D. Seweryniak, K. S. Sharma, H. Zhang, S. Zhu, Y. Zhu, [Masses and \$\beta\$ -decay spectroscopy of neutron-rich odd-odd \$^{160,162}\text{Eu}\$ nuclei: Evidence for a subshell gap with large deformation at \$n = 98\$](#) , Phys. Rev. Lett. 120 (2018) 182502. [doi:10.1103/PhysRevLett.120.182502](https://doi.org/10.1103/PhysRevLett.120.182502)
 URL <https://link.aps.org/doi/10.1103/PhysRevLett.120.182502>
- [11] R. Orford, F. G. Kondev, G. Savard, J. A. Clark, W. S. Porter, D. Ray, F. Buchinger, M. T. Burkey, D. A. Gorelov, D. J. Hartley, J. W. Klimes, K. S. Sharma, A. A. Valverde, X. L. Yan, [Spin-trap isomers in deformed, odd-odd nuclei in the light rare-earth region near \$n = 98\$](#) , Phys. Rev. C 102 (2020) 011303. [doi:10.1103/PhysRevC.102.011303](https://doi.org/10.1103/PhysRevC.102.011303)
 URL <https://link.aps.org/doi/10.1103/PhysRevC.102.011303>
- [12] G. Bollen, S. Becker, H.-J. Kluge, M. König, R. Moore, T. Otto, H. Raimbault-Hartmann, G. Savard, L. Schweikhard, H. Stolzenberg, [Isoltrap: a tandem penning trap system for accurate on-line mass determination of short-lived isotopes](#), Nuclear Instruments and Methods in Physics Research Section A: Accelerators, Spectrometers, Detectors and Associated Equipment 368 (3) (1996) 675–697. [doi:https://doi.org/10.1016/0168-9002\(95\)00561-7](https://doi.org/10.1016/0168-9002(95)00561-7)
 URL <https://www.sciencedirect.com/science/article/pii/0168900295005617>
- [13] S. Eliseev, K. Blaum, M. Block, A. Dörr, C. Droese, T. Eronen, M. Goncharov, M. Höcker, J. Ketter, E. M. Ramirez, D. A. Nesterenko, Y. N. Novikov, L. Schweikhard, [A phase-imaging technique for cyclotron-frequency measurements](#), Applied Physics B 114 (1) (2014) 107–128. [doi:10.1007/s00340-013-5621-0](https://doi.org/10.1007/s00340-013-5621-0)
 URL <https://doi.org/10.1007/s00340-013-5621-0>
- [14] R. Orford, J. Clark, G. Savard, A. Aprahamian, F. Buchinger, M. Burkey, D. Gorelov, J. Klimes, G. Morgan, A. Nystrom, W. Porter, D. Ray, K. Sharma, [Improving the measurement sensitivity of the Canadian Penning Trap mass spectrometer through PI-ICR](#), Nuclear Instruments and Methods in Physics Research Section B: Beam Interactions with Materials and Atoms 463 (2020) 491–495. [doi:https://doi.org/10.1016/j.nimb.2019.04.016](https://doi.org/10.1016/j.nimb.2019.04.016)
 URL <https://www.sciencedirect.com/science/article/pii/S0168583X19302009>
- [15] G. Savard, M. Brodeur, J. Clark, R. Knaack, A. Valverde, [The \$n=126\$ factory: A new facility to produce very heavy neutron-rich isotopes](#), Nuclear Instruments and Methods in Physics Research Section B: Beam Interactions with Materials and Atoms 463 (2020) 258–261. [doi:https://doi.org/10.1016/j.nimb.2019.05.024](https://doi.org/10.1016/j.nimb.2019.05.024)
 URL <https://www.sciencedirect.com/science/article/pii/S0168583X19303295>
- [16] R. Vondrasek, A. Levand, R. Pardo, G. Savard, R. Scott, [Charge breeding results and future prospects with electron cyclotron resonance ion source and electron beam ion source](#), Review of Scientific Instruments 83 (2) (2012) 02A913. [doi:https://doi.org/10.1063/1.3673629](https://doi.org/10.1063/1.3673629)
- [17] F. Kondev, M. Wang, W. Huang, S. Naimi, G. Audi, [The NUBASE2020 evaluation of nuclear physics properties](#), Chinese Physics C 45 (3) (2021) 030001. [doi:10.1088/1674-1137/abddae](https://doi.org/10.1088/1674-1137/abddae)
 URL <https://doi.org/10.1088/1674-1137/abddae>
- [18] G. Savard, A. Levand, B. Zabransky, [The CARIBU gas catcher](#), Nuclear Instruments and Methods in Physics Research Section B: Beam Interactions with Materials and Atoms 376 (2016) 246–250, proceedings of the XVIIth International Conference on Electromagnetic Isotope Separators and Related Topics (EMIS2015), Grand Rapids, MI, U.S.A., 11–15 May 2015. [doi:https://doi.org/10.1016/j.nimb.2016.02.050](https://doi.org/10.1016/j.nimb.2016.02.050)
 URL <https://www.sciencedirect.com/science/article/pii/S0168583X16001804>
- [19] C. N. Davids, D. Peterson, [A compact high-resolution isobar separator for the caribu project](#), Nuclear Instruments and Methods in Physics Research Section B: Beam Interactions with Materials and Atoms 266 (19) (2008) 4449–4453, proceedings of the XVth International Conference on Electromagnetic Isotope Separators and Techniques Related to their Applications. [doi:https://doi.org/10.1016/j.nimb.2008.05.148](https://doi.org/10.1016/j.nimb.2008.05.148)
 URL <https://www.sciencedirect.com/science/article/pii/S0168583X08007544>
- [20] T. Y. Hirsh, N. Paul, M. Burkey, A. Aprahamian, F. Buchinger, S. Caldwell, J. A. Clark, A. F.

- Levand, L. L. Ying, S. T. Marley, G. E. Morgan, A. Nystrom, R. Orford, A. P. Galván, J. Rohrer, G. Savard, K. S. Sharma, K. Siegl, **First operation and mass separation with the CARIBU MR-TOF**, Nuclear Instruments and Methods in Physics Research Section B: Beam Interactions with Materials and Atoms 376 (2016) 229–232, proceedings of the XVIIth International Conference on Electromagnetic Isotope Separators and Related Topics (EMIS2015), Grand Rapids, MI, U.S.A., 11-15 May 2015. [doi:<https://doi.org/10.1016/j.nimb.2015.12.037>](https://doi.org/10.1016/j.nimb.2015.12.037)
- URL <https://www.sciencedirect.com/science/article/pii/S0168583X15012835>
- [21] Heat Wave Labs - Alkali earths and Alkali metal, https://www.cathode.com/i_alkali.htm#table_a.
- [22] M. Wang, W. Huang, F. Kondev, G. Audi, S. Naimi, **The AME 2020 atomic mass evaluation (II). tables, graphs and references**, Chinese Physics C 45 (3) (2021) 030003. [doi:10.1088/1674-1137/abddaf](https://doi.org/10.1088/1674-1137/abddaf).
- URL <https://doi.org/10.1088/1674-1137/abddaf>
- [23] G. Li, S. Caldwell, J. A. Clark, S. Gulick, A. Hecht, D. D. Lascar, T. Levand, G. Morgan, R. Orford, G. Savard, K. S. Sharma, J. Van Schelt, **A compact cryogenic pump**, Cryogenics 75 (2016) 35–37. [doi:<https://doi.org/10.1016/j.cryogenics.2015.12.006>](https://doi.org/10.1016/j.cryogenics.2015.12.006)
- URL <https://www.sciencedirect.com/science/article/pii/S0011227515001691>
- [24] RoentDek Handels GmbH - MCP Delay Line Detector Manual version 11.0.2107.1, <http://www.roentdek.com/manuals/>.
- [25] D. Ray, Mass measurements of neutron-rich nuclides for the astrophysical r process using the canadian penning trap mass spectrometer, Ph.D. thesis, University of Manitoba (2022).
- [26] C. Weber, D. Ray, A. Valverde, J. Clark, K. Sharma, **Gaussian mixture model clustering algorithms for the analysis of high-precision mass measurements**, Nuclear Instruments and Methods in Physics Research Section A: Accelerators, Spectrometers, Detectors and Associated Equipment 1027 (2022) 166299. [doi:<https://doi.org/10.1016/j.nima.2021.166299>](https://doi.org/10.1016/j.nima.2021.166299)
- URL <https://www.sciencedirect.com/science/article/pii/S0168900221011190>
- [27] G. Bollen, R. Moore, G. Savard, H. Stolzenberg, The accuracy of heavy-ion mass measurements using time of flight-ion cyclotron resonance in a penning trap, Journal of Applied Physics 68 (9) (1990) 4355–4374. [doi:<https://doi.org/10.1063/1.346185>](https://doi.org/10.1063/1.346185)
- [28] M. Brodeur, V. Ryjkov, T. Brunner, S. Ettenauer, A. Gallant, V. Simon, M. Smith, A. Lapierre, R. Ringle, P. Delheij, et al., Verifying the accuracy of the titan penning-trap mass spectrometer, International journal of mass spectrometry 310 (2012) 20–31.
- [29] Stahl Electronics - BS Series ultra high precision voltage sources, <https://www.stahl-electronics.com/voltage-source.html>.
- [30] D. E. M. Hoff, K. Kolos, G. W. Misch, D. Ray, B. Liu, A. A. Valverde, M. Brodeur, D. P. Burdette, N. Callahan, J. A. Clark, A. T. Gallant, F. G. Kondev, G. E. Morgan, M. R. Mumpower, R. Orford, W. S. Porter, F. Rivero, G. Savard, N. D. Scielzo, K. S. Sharma, K. Sieja, T. M. Sprouse, L. Varriano, **Direct mass measurements to inform the behavior of ^{128m}Sb in nucleosynthetic environments**, Phys. Rev. Lett. 131 (2023) 262701. [doi:10.1103/PhysRevLett.131.262701](https://doi.org/10.1103/PhysRevLett.131.262701)
- URL <https://link.aps.org/doi/10.1103/PhysRevLett.131.262701>
- [31] A. A. Valverde, F. G. Kondev, B. Liu, D. Ray, M. Brodeur, D. P. Burdette, N. Callahan, A. Cannon, J. A. Clark, D. E. M. Hoff, R. Orford, W. S. Porter, K. S. Sharma, L. Varriano, Precise mass measurements of $a = 133$ isobars with the canadian penning trap: Resolving the q_{β^-} anomaly at ^{133}Te (2024). [arXiv:2312.06903](https://arxiv.org/abs/2312.06903).
- [32] A. J. Mitchell, R. Orford, G. J. Lane, C. J. Lister, P. Copp, J. A. Clark, G. Savard, J. M. Allmond, A. D. Ayangeakaa, S. Bottoni, M. P. Carpenter, P. Chowdhury, D. A. Gorelov, R. V. F. Janssens, F. G. Kondev, U. Patel, D. Seweryniak, M. L. Smith, Y. Y. Zhong, S. Zhu, **Ground-state and decay properties of neutron-rich ^{106}Nb** , Phys. Rev. C 103 (2021) 024323. [doi:10.1103/PhysRevC.103.024323](https://doi.org/10.1103/PhysRevC.103.024323)
- URL <https://link.aps.org/doi/10.1103/PhysRevC.103.024323>
- [33] R. Ringle, G. Bollen, A. Prinke, J. Savory, P. Schury, S. Schwarz, T. Sun, **A “lorentz” steerer for ion injection into a penning trap**, International Journal of Mass Spectrometry 263 (1) (2007) 38–44. [doi:<https://doi.org/10.1016/j.ijms.2006.12.008>](https://doi.org/10.1016/j.ijms.2006.12.008)
- URL <https://www.sciencedirect.com/science/article/pii/S1387380606005781>